Available online at www.CivileJournal.org

Civil Engineering Journal

(E-ISSN: 2476-3055; ISSN: 2676-6957)

Vol. 10, No. 01, January, 2024

The behavior of Shear Connectors in Steel-Normal Concrete Composite Structure under Repeated Loads

Abdulamir A. Karim [1], Jawad Abd Matooq [1*], Oday A. Abdulrazzaq [1], Fareed Hameed Majeed [1], Samoel Mahdi Saleh [1]

[1] *Department of Civil Engineering, College of Engineering, University of Basrah, Iraq.*

Received 30 September 2023; Revised 15 December 2023; Accepted 21 December 2023; Published 01 January 2024

Abstract

In today's construction industry, the use of composite beams is becoming more and more important, particularly for long-span bridges that must withstand repeated loads from moving automobiles. This work investigates the behavior of composite beams through experimentation. Six push-out steel-concrete specimens are made and tested with various levels of static and repetitive loading applied. The specimens are made of rolled steel sections that are joined to concrete decks on both sides by stud shear connectors. Two approaches—one static and the other repeating—applied a push-out load to two sets of samples. One has a stud shear connector measuring 16 mm, and the other measures 25 mm. Three specimens were made for each group. To determine the final load, one specimen from each group underwent a static push-out test in the first stage. In the subsequent phase, repeated loads of 0-80% and 25-80% of the maximum static load were applied to the remaining ones. The analysis process measured the variation in slip between the concrete decks and the steel section over several load cycles. It was found that the recorded slip values at the ultimate load increased about four times just before the failure. The recorded values of the residual slip at the end of each load cycle decreased with the increase in load cycle numbers. Also, it was found that the values of the residual slip depend on the values of the lower and upper limits of the load level.

Keywords: Composite Beams; Push-Out Test; Repeated Load; Residual Strength; Load Slip Relation; Composite Construction.

1. Introduction

Composite construction constitutes one of the most cost-efficient structural systems by using the desired properties of various materials in an optimal manner. Concrete decks or slabs connected to rolled steel sections are widely used in the applications of long-span bridges and floors. The rolled steel sections are connected to concrete slabs using mechanical devices called shear connectors to transfer the horizontal axial forces between the two components to ensure their integrity. The use of shear connectors between steel beams and concrete slabs appeared in the 1950s rather than the design of each component to behave separately, keeping in mind the design of steelwork to carry the whole weight of the concrete [1].

Many types of shear connectors were developed, such as steel bars and tees with hoops, channels, angles, and stud shear. The stud shear is proven to behave as a ductile member, so it is most widely used with a practical length of 65 to 150 mm and a diameter of 13 to 25 mm, although larger dimensions are also found [1]. So most experimental and theoretical research was focused on composite beams with headed stud shear connectors.

* Corresponding author: jawad.abd-matooq@uobasrah.edu.iq

http://dx.doi.org/10.28991/CEJ-2024-010-01-013

Jayas & Hosain [2] tested composite beams of full-size and push-out specimens to investigate the mode of failure. They found that pull-out was the dominant mode of failure. They also developed an empirical formula to estimate the ultimate shear strength and bending moment. Ellobody & Young [3] used the finite element method to create a nonlinear model that represents a composite system consisting of a concrete slab with profiled steel sheeting connected by headed studs orthogonal to a steel beam. They found that the shear capacity calculated based on the design criteria in the British and American codes was higher, while that calculated based on the European Code was lower compared to that found by their nonlinear analysis. Similar findings were obtained by the finite element analysis conducted by Bonilla et al. [4] and the experimental work of Hicks & Smith [5] on a composite system consisting of a steel beam, a concrete slab, and profiled steel sheeting. Albarram [6] used ABAQUS to conduct a 3-D finite element analysis of a composite beam with a very deep-profiled steel deck. He found that the shear strength of headed stud connectors for 100 to 146 mm decks was about 65% of that for beams with ordinary decks. Shim et al. (2010) [7] investigated by experimental tests and finite element analysis using ANSYS the shear strength and the load-slip relationship of stud connectors embedded in fiber-reinforced concrete and high-strength concrete slabs. They found that the equations given for normal concrete need to be modified to be applied to high-strength concrete. A numerical model for the push-out tests was proposed by Bouchair et al. [8] using the available experimental works to verify its validity.

Qureshi et al. [9] examined the validity of various three-dimensional finite element models using static and dynamic analysis procedures that appropriately estimate the shear strength and the post-failure behavior of composite beams with stud shear connectors and profiled steel sheeting. The results were compared with the available experimental work. They found that the Concrete-Damaged Plasticity model can reasonably predict the shear capacity and the post-failure behavior. Jayanthi & Umarani [10] conducted a series of push-out tests on fifteen composite beams of steel and concrete using five types of shear connectors: stud connector, channel connector, I-connector, S-connector, and Z-connector. The work aimed to evaluate the load-slip relationship and failure mechanisms for the various types. The results revealed that no pull-off failure was noticed for all types of connectors, and the channel connectors had a higher capacity compared to the other types.

Choi & Kim [11] performed push-out tests on thirteen specimens to investigate the effect of beam geometry and the steel anchor types on the behavior of the specimens. They found that the types of steel anchors have more effect compared to the geometry of the steel beams. Arévalo et al. [12] studied the behavior of fourteen specimens of composite steel-concrete beams using two sets of 45˚ and 90˚ angled steel shear connectors under the effects of the push-out test, monotonic loads, and repeated loads. They found that specimens of the 45˚angled group had better results compared to those of the 90˚ angled group. Saleh & Majeed [13] carried out the push-out test on 36 specimens of composite beams consisting of steel sections connected to self-compacting concrete slabs made of recycled aggregate using stud connectors. They found that the presence of recycled aggregate decreases the shear capacity of stud connectors, shear stiffness, and the ultimate slip. The effect of repeated loading on the ductility of reinforced concrete beams with embedded I-sections has been explored by Ibrahim & Allawi [14]. Two materials for the embedded I-section were examined using steel and GFRP. Five cycles of loading and unloading of up to 75% of the static ultimate load were applied to the composite beams with and without shear connectors. Zhao et. al. [15] proposed a one-dimensional finite element model to explore the slip and shear lag of composite box girders under the action of time-dependent loading. Zhao et. al. [16] used ABAQUS software to model the behavior of composite beams of various types under the action of impact loads.

2. Fatigue Strength

The effect of fatigue loading on the performance of composite beams was explored in several previous works to determine the effect of repeated loads on shear capacity and load slip relations. Bro & Westberg [17] conducted static and fatigue push-out tests to investigate the influence of the fatigue load on the shear capacity of the stud connectors. They found that the shear capacity decreases as the loading cycles increase.

Lee et al. [18] investigated, using static and fatigue push-out tests, the behavior of composite beams using shear studs of up to 30 mm diameter, which were greater than allowed by design codes. It was found that the experimental fatigue strength is slightly lower than that specified by Eurocode-4 and AASHTO LRFD. Hanswille et al. [19] used cycles of unidirectional push-out tests with different loading sequences to explore the fatigue life and the drop in static strength of 71 specimens of composite beams. They found that the static capacity of the specimens was reduced because of the cracks at the root of the studs, which started to appear in about 15% of the fatigue life. In their companion work [20], they developed an analytical procedure for predicting the fatigue life of shear connectors by using the static strength, peak loading, and range of loading cycles.

Azad et al. [21] proposed a procedure to extend the method of determining the fatigue life load of composite beams with full interaction to be used to predict the fatigue life load of composite beams with partial interaction. It was concluded that using slips gave more accurate results than using stresses. Also, the required number of shear connectors could be decreased if connectors with better fatigue properties were implemented. The slip between the steel section and concrete deck of composite beams subjected to fatigue loading was explored by Liang et al. [22]. Push-out specimens were tested under the action of static and repeated loads, and the cumulative and residual slips were measured.

The present work will explore the fatigue life load and load slip relation for composite beams made of a rolled steel section and two reinforced concrete slabs, all connected using headed stud shear connectors. The main parameters considered are the concrete strength, the diameter of shear connectors, and the loading sequence.

3. Fabrication of Test Specimens

Six specimens are composed of steel beams connected at both flanges to concrete slabs via headed stud shear connectors, as shown in Figure 1. In three specimens, 25-mm-headed studs were used as shear connectors, while in the remaining three specimens, 16-mm-headed studs were used. All other properties are identical in all test specimens. The dimensions and material properties of specimens are listed in Table 1. The dimensions of stud shear connectors conform to the requirements of Eurocode 4 [23], in which the height is greater than three times the shank diameter and the head diameter and depth are not less than 1.5 and 0.4 of the shank diameters, respectively.

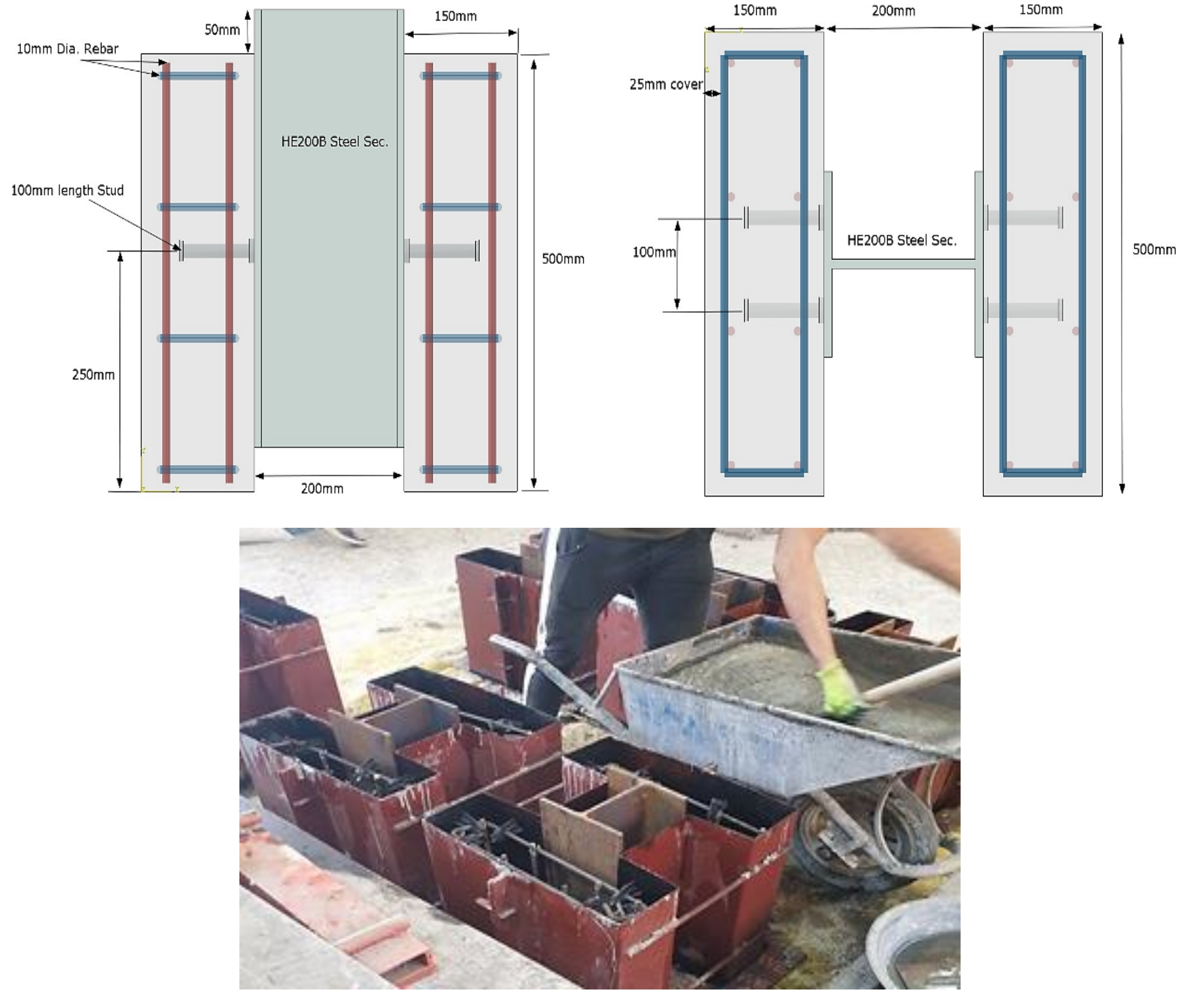

Figure 1. Form and reinforcement of a push-out test specimen

Table 1. Dimensions and properties of steel section and concrete deck

Group ID	Steel Beam		Concrete Decks			Stud Shear Connectors			
	Rolled section	Grade	Width (mm)	Thickness (mm)	Compression strength (MPa)	Diameter (mm)		Height (mm)	Grade
						shank	head		
S1-D25	HE200B	375	500	150	32.4	25	35	100	500
S2-D16						16	25	100	500

4. Materials Used

Concrete and steel are obtained by selecting suitable and under good quality control materials. Figure 2 represents the granulation diagram for the used materials.

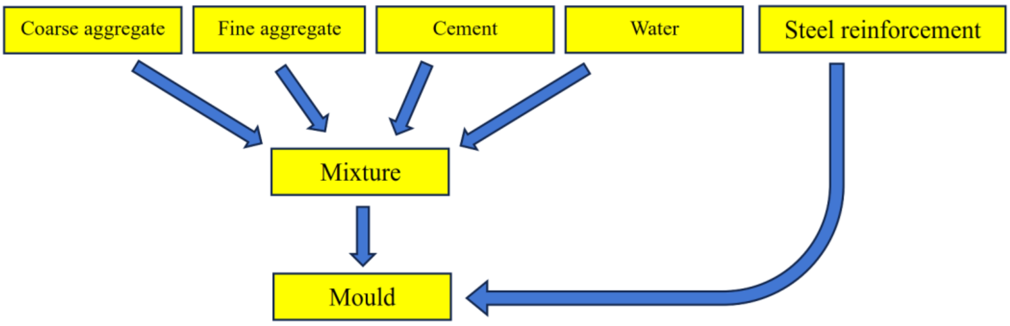

Figure 2. The granulation diagram for the used materials

4.1. Cement

Ordinary Portland cement available in local markets was used in this work. Table 2 lists the compound and chemical properties of the cement used in the present study. The physical properties of cement are listed in Table 3. As shown from the test results, the cement used conforms with the requirements of the ASTM C150-15 specification [24].

Table 2. Chemical composition and main compounds of cement

Oxide Composition	% by weight	Requirements of ASTM C150-15
MgO	2.15	Not more than 6.0
CaO	63.17	--------
Fe2O3	4.3	--------
C3A	2.85	Not more than 3.0
SO3	2.13	--------
C4AF	13.86	Not more than 25.0
Residue of insoluble	0.58	Not more than 0.75
Loss on ignition	2.31	Not more than 3.0

Table 3. Physical properties of the used cement

Physical properties	Test result	Requirements of ASTM C150-15
Initial setting time (Using Vicat method) (min)	130	More than 45
Final setting time (Using Vicat method) (min)	290	Less than 375
Specific surface area (Using Blaine Method) (m^2/kg)	310	not less than 2^0
Compressive strength at 3-days (MPa)	15.6	More than 12
Compressive strength at 7-days (MPa)	23.4	More than 19

4.2. Fine Aggregate

Natural sand from the Jabal Sanam region in the south of Iraq was used, which has a fineness modulus (F.M.) of 2.87. Table 4 shows the sieve analysis for the sand and the requirements of ASTM C33-13 [25]. The properties of the fine aggregate are listed in Table 5.

Table 4. Grading of fine aggregate

Sieve size (mm)	Passing (%)	ASTM C33-13 Limits (%)
9.5	100	100
4.75	98	95-100
2.36	88	80-100
1.18	68	50-85
0.600	48	25-60
0.300	18	5-30
0.150	0	0-10

Table 5. Properties of fine aggregate

Property	Test result
Specific gravity	2.63
Absorption	0.97%
Sulfate content	0.10%

4.3. Coarse Aggregate

Natural crushed gravel of maximum size (12.5 mm) from the Jabal Sanam region was used. Table 6 shows the grading of this aggregate, which conforms to ASTM C33-13 [25]. The properties of the coarse aggregate are listed in Table 7.

Table 6. Grading of coarse aggregate

Sieve Size (mm)	Passing by weight (%)	ASTM C33-03 LIMITS (%)
19	100	100
12.5	95	90-100
9.5	60	40-70
4.75	6	0-15
2.36	2	0-5

Table 7. Properties of coarse aggregate

Property	Test result
Specific gravity	2.61
Absorption	1.10%
Sulfate content	0.062%

The weights of materials used in producing the concrete mix per one cubic meter are listed in Table 8, where potable water was used for both mixing and curing of concrete.

Table 8. Contents of the concrete mix

Cement (kg/m^3)	Fine aggregate (kg/m^3)	Coarse aggregate (kg/m^3)	Water (kg/m^3)	W/C ratio
420	672	1176	189	0.45

4.4. Steel Reinforcement

Deformed reinforcing steel bars were used in this study with a nominal diameter of 10.0 mm. The properties of the rebars used are listed in Table 9.

Table 9. Properties of the rebars

Diameter (mm)	Yield stress (MPa)	Ultimate strength (MPa)	Elongation (%)
10	440	630	11

5. Testing of Hard Concrete

5.1. Compressive Strength (f'_c)

Three cylindrical specimens with a diameter of 150 mm and a height of 300 mm were cast according to ASTM C 873-10a [26]. The average compressive strength for the three specimens is 32.5 MPa.

5.2. Static Modulus of Elasticity (E)

The static-elastic modulus for concrete was found according to ASTM C469-14 [27]. Three cylindrical specimens with a diameter of 150 mm and a height of 300 mm were tested to find the average value of the modulus of elasticity, which was equal to 30.1 GPa.

5.3. Splitting Tensile Strength (f_t)

Three cylindrical specimens of 150 mm and a height of 300 mm were tested according to ASTM C496-11 [28] to find splitting tensile strength, where the average tensile splitting strength for those specimens was 3.6 MPa.

6. Push-out Test of Composite Beam Specimens

6.1. Methodology

The sequence of testing specimens can be briefly described by the flow chart shown in Figure 3.

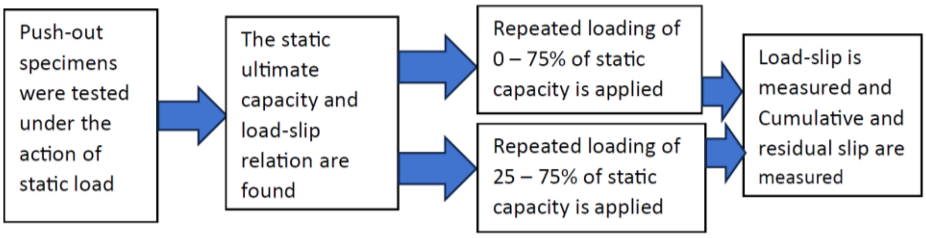

Figure 3. Testing sequence

6.2. Ultimate Strength Test

As mentioned above, test specimens were categorized into two groups deferred to each other by the size of the shear connectors implemented to maintain the composite action between a steel beam lying in the middle of two concrete decks. One sample of each group (S2-D16 and S1-D25) was used to find the ultimate load capacity of the pertaining group. This was done by implementing the ordinary push-out test, in which a gradually increasing load is applied to the steel beam, which transfers the load through shear connectors to the concrete decks on both sides, which transfers the load to the supports. The average slip that occurred between the beam and decks was measured and recorded for each loading step, as shown in Figure 4. A comparison of the relation between the applied load and the slip between steel and concrete for the two specimens is shown in Figure 5. From this figure, it can be shown that the relation for each specimen is linear up to a certain value of the applied load. For specimen (S1-D25), the linear relation was noted to be an applied load of about 360 kN, while for specimen (S2-D16), this load was about 320 kN. The load slip relation then changed to ascending rapid curvature until a maximum capacity of 503.3 kN and 366.2 kN for S1-D25 and S2-D16, respectively, was reached, after which the relation turned to a descending curve. Figure 5 shows the linear relations of the ultimate load were maintained at about 71.5% for S1-D25 and 87.4% for S2-D16, respectively. The slip at the ultimate capacity was found to be 4.38 mm for S1-D25 and 3.32 mm for S2-D16. After the ultimate loads, the studs exhibit considerable ductility with increasing slip until failure, where the maximum recorded slip at the failure loads was 17.67 mm and 14.14 mm for S1-D25 and S2-D16, respectively. The slip values recorded at failure loads compared to ultimate loads increased by about 4.03 times for S1-D25 and 4.26 times for S2-D16 specimens.

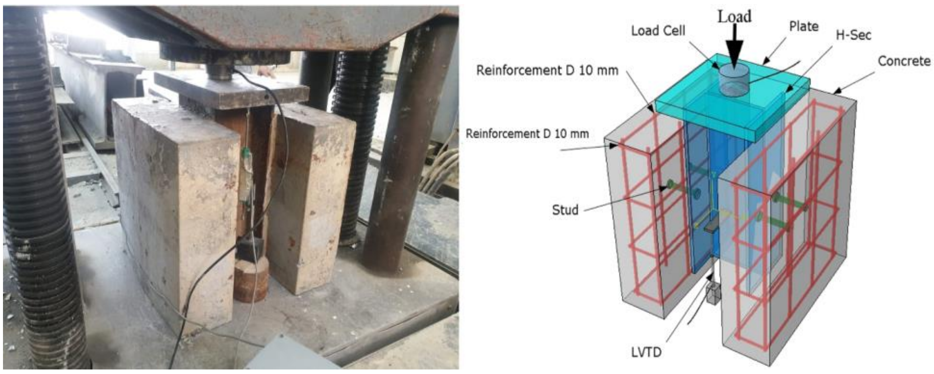

Figure 4. Push-out test specimen setup

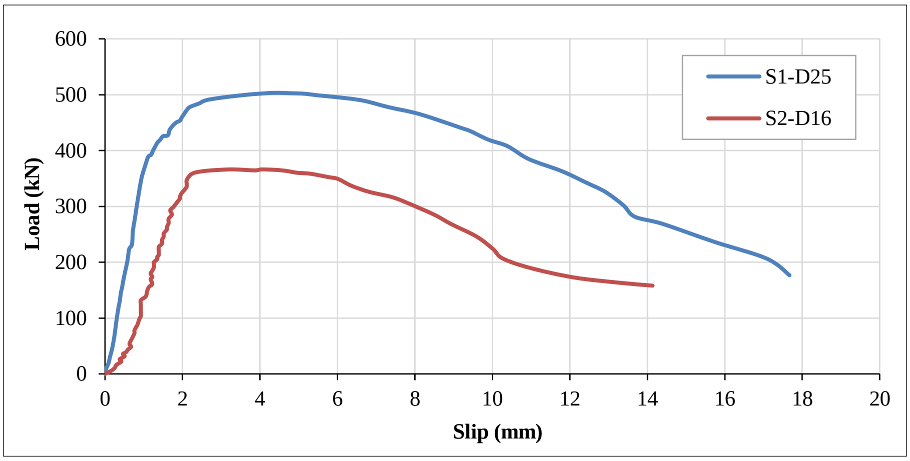

Figure 5. Load slip relations for push-out specimens

6.3. Residual Strength

To determine the deterioration of strength due to fatigue, a unidirectional repeated loading was applied to two specimens from each group. The loading procedure was performed by two approaches; the first was to subject the samples to repeated loads with an amplitude ranging from 0 to 75% of the ultimate strength, whereas the loading amplitude in the second approach ranged from 25 to 75% of the ultimate strength. The ultimate strength was already found for each group by the traditional static push-out test, as previously mentioned. The repeated load was applied by using a digital actuator connected to a universal hydraulic testing machine. A repeated load was applied by exerting a displacement rate of about 0.005 mm/min. The load applied at any instant, together with the slip displacement of the steel beam relative to concrete decks measured by a digital transducer, were recorded instantaneously, as shown in Figure 4.

The variation of slip displacement with the applied load for the various loading cycles from the repeated loading test is shown in Figures 6 to 9. Figures 6 and 7 show the test output for specimens of groups S1-D25 and S2-D16, respectively, subjected to loading amplitudes varying from 0 to 75% of the ultimate load. The relevant results for the case of 25 to 75% amplitude of repeated loading are shown in Figures 8 and 9.

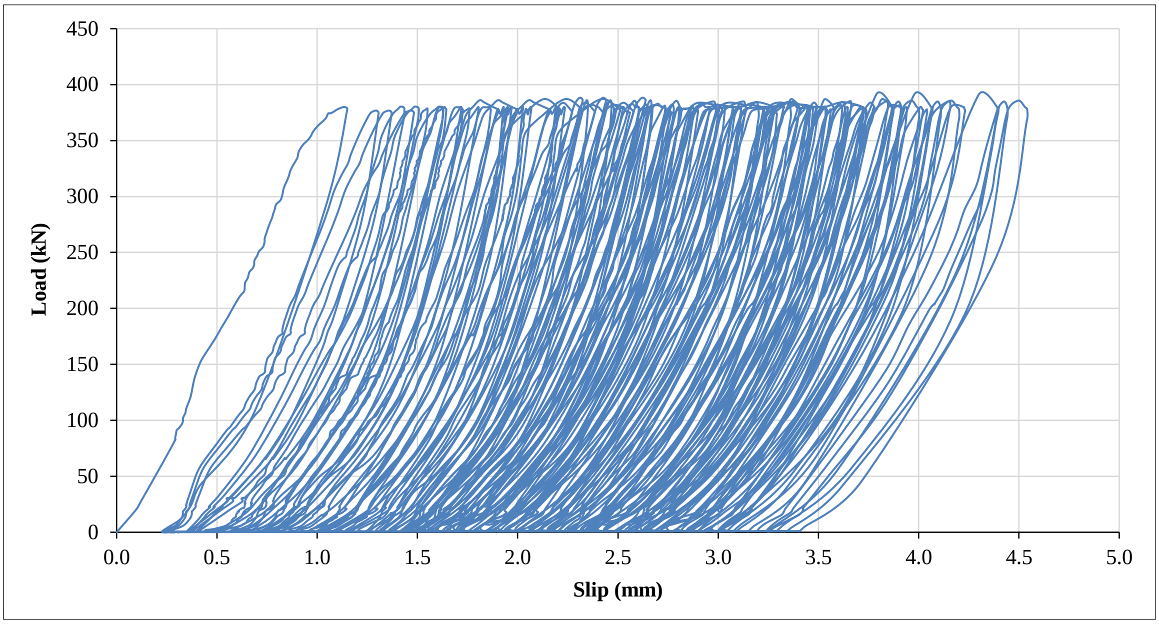

Figure 6. Repeated loading test for S1-D25, for 0-75% amplitude

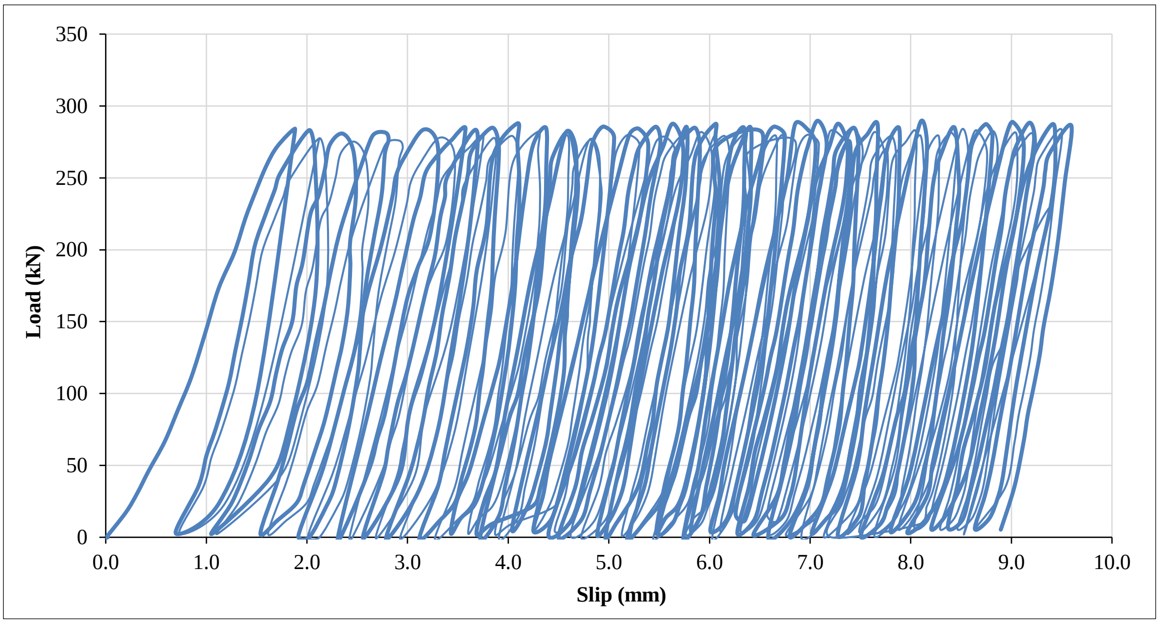

Figure 7. Repeated loading test for S2-D16, for 0-75% amplitude

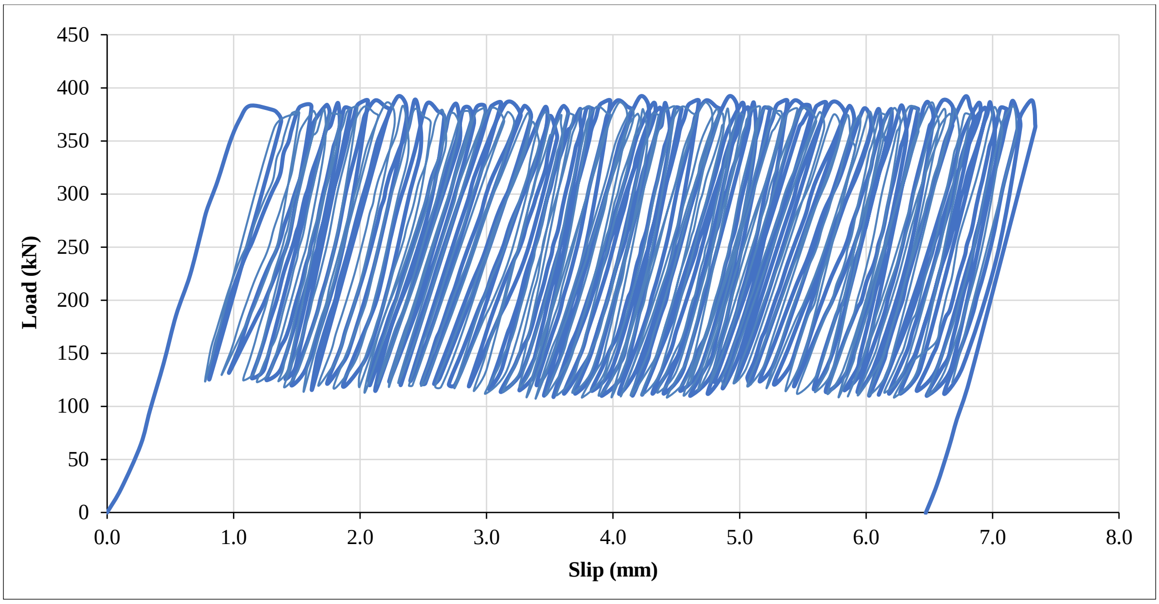

Figure 8. Repeated loading test for S1-D25, for 25-75% amplitude

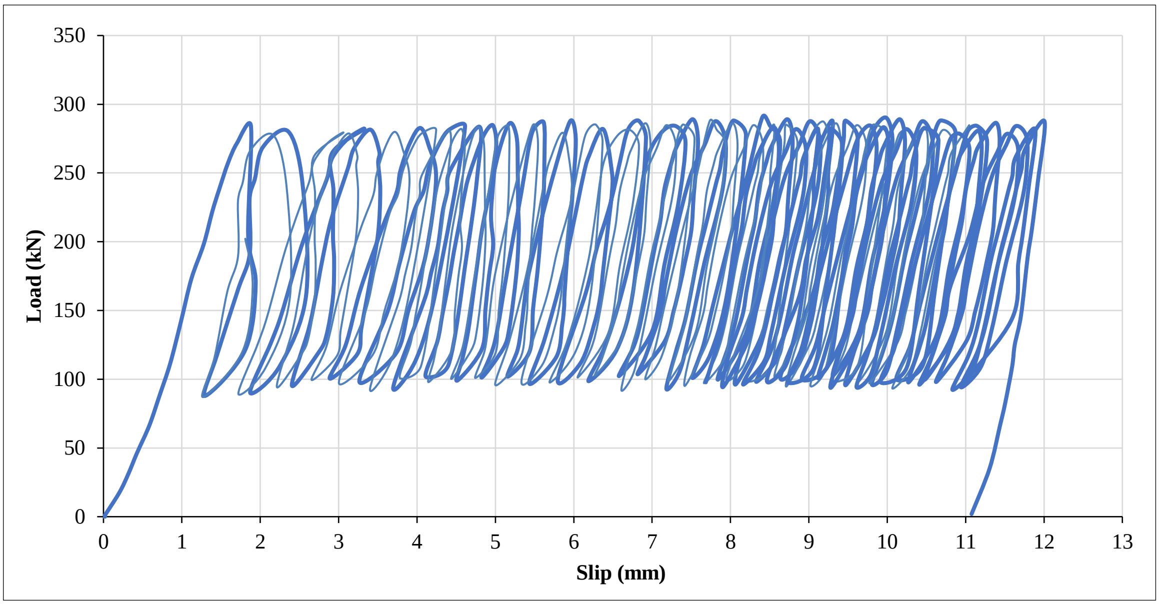

Figure 9. Repeated loading test for S2-D16, for 25-75% amplitude

From these variations, it could be observed that the slope of the load-slip curve increases with the increase in loading cycle numbers; this indicates that the stiffness of the composite beams increases with each loading cycle. It is noticeable that the slope of the load-slip curve is lower for specimens of group S1-D25 as compared to specimens of group S2-D16 during the two cases of loading cycles of 0 to 57% and 25 to 75%. Figures 6 to 9 illustrate that the increasing rate of slip values for group S1-D25 is less compared to that of group S2-D16 as the number of loading cycles increases. When the applied load completely vanishes or reduces to 25% of the ultimate load, a certain value of slip permanently remains between the steel beam and the contact concrete slabs.

6.4. Residual Slip

The relations between slip values that lag after each loading cycle and the number of loading cycles for the two cases of loading cycles (0 to 75%) and (25 to 75%) of the ultimate loads are shown in Figures 10 to 13 for specimens of groups (S1-D25) and (S2-D16). From these figures, it could be noted that the residual slip after the first loading cycle for each case is significantly greater than the residual slip remaining after any of the later cycles. For both groups of tested specimens, the residual slip for the loading case amplitude of 25 to 75% of the ultimate load is greater than that of the loading case of 0 to 75%. This indicates that the residual slip increases as the value of the lower limit of the loading amplitude increases, in addition to its dependence on the upper limit of that amplitude. For specimens of group S1-D25, the recorded residual slip values after each loading cycle were less compared to the recorded values of group S2-D16 for both cases of the loading cycles, whether it was 0 to 75% or 25 to 75% of the ultimate load.

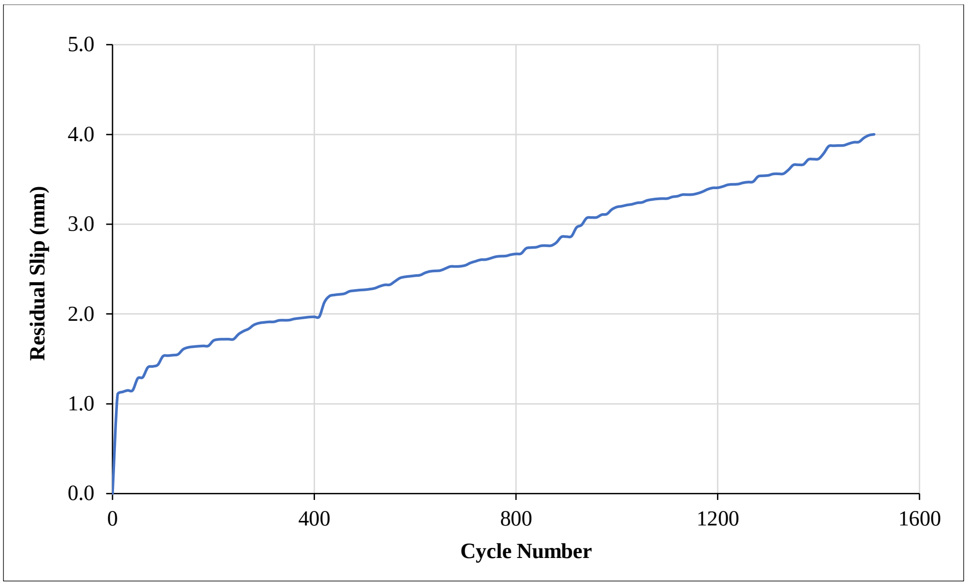

Figure 10. Repeated loading test for S1-D25, for 0-75% Amplitude

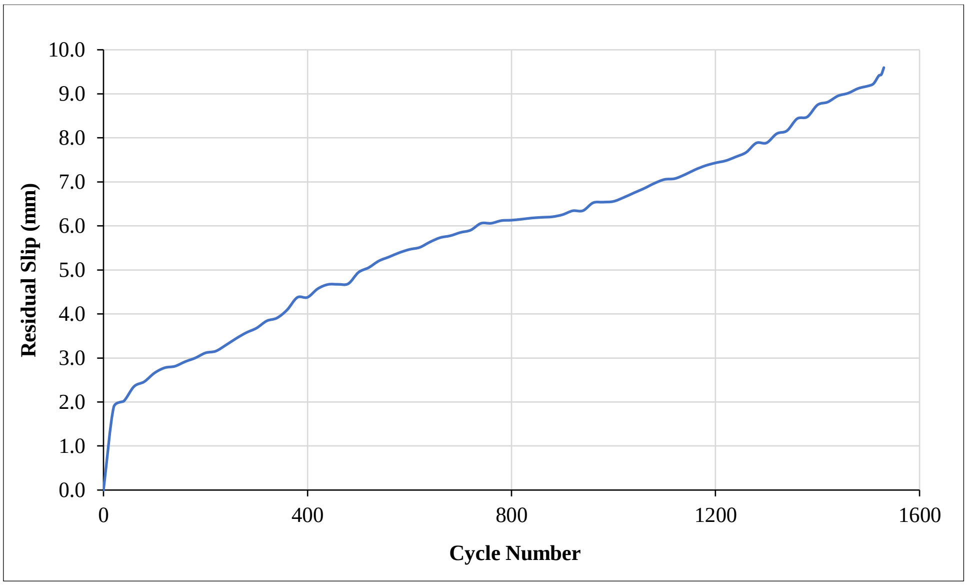

Figure 11. Repeated loading test for S2-D16 for 0-75% Amplitude

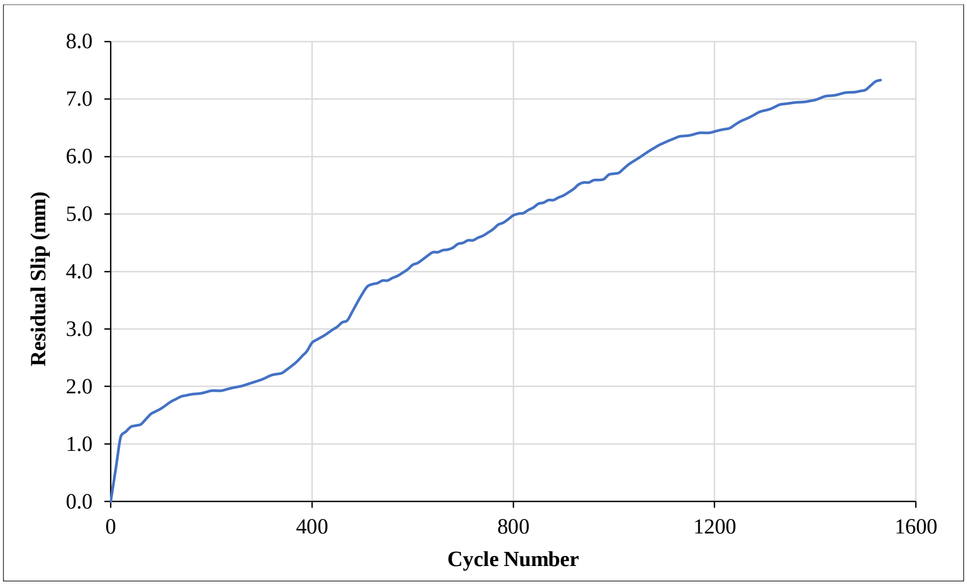

Figure 12. Repeated loading test for S1-D25, for 25-75% Amplitude

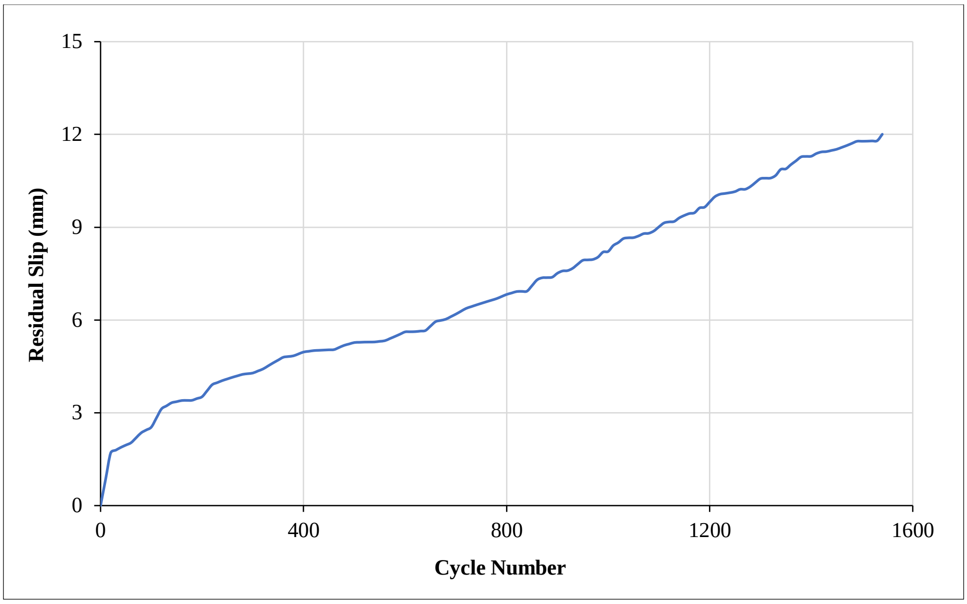

Figure 13. Repeated loading test for S2-D16 for 25-75% Amplitude

7. Conclusions

To explore the behavior of composite beams under repeated loads, six push-out steel-concrete specimens composed of a rolled steel section connected to concrete slabs on both sides by stud shear connectors are fabricated and tested under the action of static and repeated loads of varying amplitudes.

Under the effect of static load, it was found that using 25 mm headed studs to connect the rolled steel section to concrete slabs resulted in a 37.4% increase in the ultimate load capacity compared to the specimens in which 16 mm headed studs were used. The relationship between the applied load and its corresponding slip is linear up to 71.5% of the ultimate load for specimens with 25mm stud shear connectors. On the other hand, for specimens with 16-mm studs, this relationship remains linear up to 87.4% of the ultimate load. In the case of using 25mm shear connectors in the explored specimens, the slip values recorded at failure loads increased about 4.03 times compared to ultimate loads, while they increased about 4.26 times in the case of using 16mm shear connectors.

Under the effect of repeated loading, the increasing rate of slip values with increasing numbers of loading cycles is less for specimens with 25mm stud shear connectors compared to specimens with 16mm studs. It was found that the residual slip depends on both the lower and upper limits of the loading amplitude. For specimens in which 25mm studs were used, the recorded residual slip values after each loading cycle were lower than the recorded values in specimens in which 16mm studs were used. Therefore, specimens with 25 mm shear connectors exhibit better behavior compared to those with 16 mm studs.

8. Declarations

8.1. Author Contributions

Conceptualization, A.A.K. and J.A.M.; methodology, A.A.K., J.A.M., and O.A.A.; validation, F.H.M. and S.M.S.; formal analysis, J.A.M.; writing—original draft preparation, A.A.K., J.A.M., O.A.A., F.H.M., and S.M.S.; writing—review and editing, A.A.K., J.A.M., O.A.A., F.H.M., and S.M.S. All authors have read and agreed to the published version of the manuscript.

8.2. Data Availability Statement

The data presented in this study are available on request from the corresponding author.

8.3. Funding

The authors received no financial support for the research, authorship, and/or publication of this article.

8.4. Conflicts of Interest

The authors declare no conflict of interest.

9. References

[1] Johnson, R. P. (2018). Composite Structures of Steel and Concrete. John Wiley & Sons, Hoboken, United States. doi:10.1002/9781119401353.

[2] Jayas, B. S., & Hosain, M. U. (1988). Behaviour of Headed Studs in Composite Beams: Push-Out Tests. Canadian Journal of Civil Engineering, 15(2), 240–253. doi:10.1139/l88-032.

[3] Ellobody, E., & Young, B. (2006). Performance of shear connection in composite beams with profiled steel sheeting. Journal of Constructional Steel Research, 62(7), 682–694. doi:10.1016/j.jcsr.2005.11.004.

[4] Bonilla Rocha, J. D., Arrizabalaga, E. M., Quevedo, R. L., & Recarey Morfa, C. A. (2012). Behavior and strength of welded stud shear connectors in composite beam. Revista Facultad de Ingeniería Universidad de Antioquia, 63, 93–104. doi:10.17533/udea.redin.12489.

[5] Hicks, S. J., & Smith, A. L. (2014). Stud Shear Connectors in Composite Beams that Support Slabs with Profiled Steel Sheeting. Structural Engineering International, 24(2), 246–253. doi:10.2749/101686614x13830790993122.

[6] Albarram, A. (2019). Behaviour of Headed Stud Connectors in Composite Beams with Very Deep Profiled Sheeting. Ph.D. Thesis, University of East London, London, United Kingdom.

[7] Shim, H. B., Chung, K. S., Jang, S. H., Park, S. J., & Lee, J. H. (2010). Push-out tests on shear studs in high strength concrete. 7th international conference on fracture mechanics of concrete and concrete structures (FraMCoS-7), 23-28 May, 2010, Jeju, Korea.

[8] Bouchair, A., Bujnak, J., Duratna, P., & Lachal, A. (2012). Modeling of the steel-concrete push-out test. Procedia Engineering, 40, 102–107. doi:10.1016/j.proeng.2012.07.063.

[9] Qureshi, J., Lam, D., & Ye, J. (2011). Effect of shear connector spacing and layout on the shear connector capacity in composite beams. Journal of Constructional Steel Research, 67(4), 706–719. doi:10.1016/j.jcsr.2010.11.009.

[10] Jayanthi, V., & Umarani, C. (2018). Performance evaluation of different types of shear connectors in steel-concrete composite construction. Archives of Civil Engineering 64(2), 97–110. doi:10.2478/ace-2018-0019.

[11] Choi, I. R., & Kim, C. S. (2021). Push-out tests on various steel anchors with partial-length welding in steel–concrete composite members. Applied Sciences (Switzerland), 11(1), 1–15. doi:10.3390/app11010105.

[12] Arévalo, D., Hernández, L., Gómez, C., Velasteguí, G., Guaminga, E., Baquero, R., & Dibujés, R. (2021). Structural performance of steel angle shear connectors with different orientation. Case Studies in Construction Materials, 14, e00523. doi:10.1016/j.cscm.2021.e00523.

[13] Saleh, S. M., & Majeed, F. H. (2022). Shear Strength of Headed Stud Connectors in Self-Compacting Concrete with Recycled Coarse Aggregate. Buildings, 12(5). doi:10.3390/buildings12050505.

[14] Ibrahim, T. H., & Allawi, A. A. (2023). The Response of Reinforced Concrete Composite Beams Reinforced with Pultruded GFRP to Repeated Loads. Journal of Engineering, 29(1), 158–174. doi:10.31026/j.eng.2023.01.10.

[15] Zhao, G. Y., Liu, W., Su, R., & Zhao, J. C. (2023). A Beam Finite Element Model Considering the Slip, Shear Lag, and Time-Dependent Effects of Steel–Concrete Composite Box Beams. Buildings, 13(1), 215. doi:10.3390/buildings13010215.

[16] Zhao, G. Y., Zhu, L., Liu, W., Zhao, J. C., & Huo, J. X. (2023). Numerical Study on the Effect of Interface Dynamic Damage of Steel–Concrete Composite Beam Bridge Caused by High–Frequency Impact Load. Buildings, 13(2), 545. doi:10.3390/buildings13020545.

[17] Bro, M., & Westberg, M. (2004). Influence of fatigue on headed stud connectors in composite bridges. Master Thesis, Lulea University of Technology, Luleå, Sweden.

[18] Lee, P. G., Shim, C. S., & Chang, S. P. (2005). Static and fatigue behavior of large stud shear connectors for steel-concrete composite bridges. Journal of Constructional Steel Research, 61(9), 1270–1285. doi:10.1016/j.jcsr.2005.01.007.

[19] Hanswille, G., Porsch, M., & Ustundag, C. (2007). Resistance of headed studs subjected to fatigue loading: Part I: Experimental study. Journal of Constructional Steel Research, 63(4), 475-484. doi:10.1016/j.jcsr.2006.06.035.

[20] Hanswille, G., Porsch, M., & Ustundag, C. (2007). Resistance of headed studs subjected to fatigue loading Part II: Analytical study. Journal of Constructional Steel Research, 63(4), 485–493. doi:10.1016/j.jcsr.2006.06.036.

[21] Azad, A. R. G., Mafipour, M. S., & Tatlari, S. (2018). Fatigue Behavior of Shear Connectors in Steel-Concrete Beams with Partial Interaction. 3rd International Conference on Steel & Structure, 11-12 December, 2018, Tehran, Iran.

[22] Liang, X., Yi, X., Wang, B., & Liu, X. (2022). Slip behavior of stud connectors of steel-concrete composite beams in the whole process of fatigue loading. Structures, 44, 1607–1616. doi:10.1016/j.istruc.2022.08.104.

[23] EN 1994-2. (2005). Design of composite steel and concrete structures – Part 2: General rules and rules for bridges. European Comittee for Standardization, Brussels, Belgium.

[24] ASTM C150/C150M. (2015). Standard Specification for Portland Cement. ASTM International, Pennsylvania, United States. doi:10.1520/C0150_C0150M-12.

[25] ASTM C33/C33M-11a. (2013). Standard Specification for Concrete Aggregates. ASTM International, Pennsylvania, United States. doi:10.1520/C0033_C0033M-11A.

[26] ASTM C873/C873M. (2010). Standard Test Method for Compressive Strength of Concrete Cylinders Cast in Place in Cylindrical Molds. ASTM International, Pennsylvania, United States. doi:10.1520/C0873_C0873M-10.

[27] ASTM C469/C469M-14. (2014). Standard Test Method for Static Modulus of Elasticity and Poisson's Ratio of Concrete in Compression. ASTM International, Pennsylvania, United States. doi:10.1520/C0469_C0469M-14.

[28] ASTM C496/C496M. (2011). Standard Test Method for Splitting Tensile Strength of Cylindrical Concrete Specimens. ASTM International, Pennsylvania, United States. doi:10.1520/C0496_C0496M-17.